Article

Research on CO$_2$−WAG in Thick Reservoirs: Geological Influencing Factors and Random Forest Importance Evaluation

Qiang Luo, Yunbo Li,* Hao Sun, Shangqi Liu, Yang Yu, and Zhaopeng Yang

Read Online

ACCESS | Metrics & More | Article Recommendations

ABSTRACT: In the development process of thick reservoirs, the impact of various geological factors on the effectiveness of the CO$_2$ water alternating gas (CO$_2$−WAG) flooding technology remains unclear. This paper establishes multiple CO$_2$−WAG flooding models for thick reservoirs to study the effects of sedimentary rhythm, dip angle, matrix permeability, high-permeability streaks (HPS), and barrier layers on the effectiveness of CO$_2$−WAG flooding and then uses the random forest algorithm to rank the importance of these geological factors. The results show that different geological factors have varying degrees of impact on the distribution of water and gas migration and recovery rates during the CO$_2$−WAG flooding process. The ranking of the importance of various factors obtained by reservoir numerical simulations and the random forest algorithm is HPS, sedimentary rhythm, dip angle, matrix permeability, and barrier layers. These research findings will provide effective guidance and a reference for the optimal selection of CO$_2$−WAG flooding schemes for similar thick reservoirs under different geological conditions.
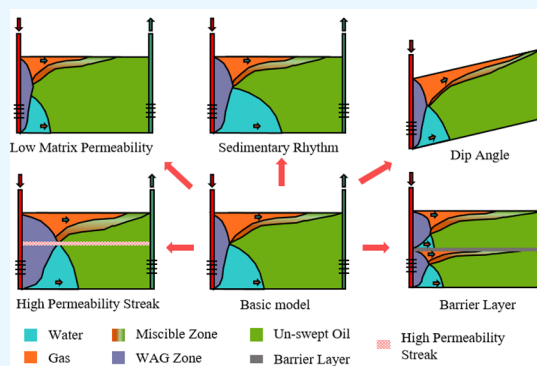
INTRODUCTION

Multiple thick reservoirs beneath the pre-salt layer have been discovered in the Santos Basin Pre-Salt Cluster (SBPSC) area.[1−3] These thick reservoirs are characterized by their significant reservoir thickness, complex geological structures, and high CO$_2$ content. Offshore operations face limitations in the gas export handling capacity. In order to efficiently handle the associated CO$_2$ gas, maintain reservoir pressure, and meet the demand for enhanced oil recovery (EOR), WAG flooding has been applied in the development of such oil fields.[4]

WAG is a technology that combines the advantages of water flooding (WF) and gas injection (GI) to enhance oil recovery.[5,6] It improves the sweep efficiency and displacement efficiency and provides better control of the displacement front stability. WAG has been successfully applied in various types of reservoirs.[7] The factors influencing the effectiveness of WAG development are mainly geological factors and injection parameters.[8−10] Additionally, as the reservoir thickness increases, the gravity segregation of injected water and gas becomes more pronounced (Figure 1), leading to diverse pathways for water and gas movement. Therefore, it is essential to conduct further research on the influencing factors of WAG, particularly in thick oil layers.

Many scholars have conducted research on the factors influencing WAG flooding from various perspectives, including laboratory experiments, numerical simulations, and field trials. Among them, numerical simulations are the most widely used due to their flexible parameter settings, cost-effectiveness, and

ease of data acquisition and observation. Table 1 presents the research findings on the influencing factors of WAG flooding by using reservoir simulation techniques. It indicates that most of the existing studies focus on reservoir thicknesses below 50 m, with CO$_2$ being the commonly injected gas. The research primarily concentrates on the optimization analysis of injection and production parameters, while geological factors such as dip angle and reservoir heterogeneity receive less attention.

Previous research on the factors influencing WAG flooding has mainly focused on the analysis and optimization of these factors, while there has been limited research on the evaluation of parameter importance, which is crucial for guiding decision-making and operations. With the continuous development of artificial intelligence technology, it has been widely applied in various fields such as healthcare, transportation, internet, and energy.[23] Random forest (RF), as a flexible artificial intelligence method,[24−26] is capable of handling complex data types and high-dimensional data, and it can provide variable importance measures (VIM).[27] Therefore, it has
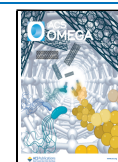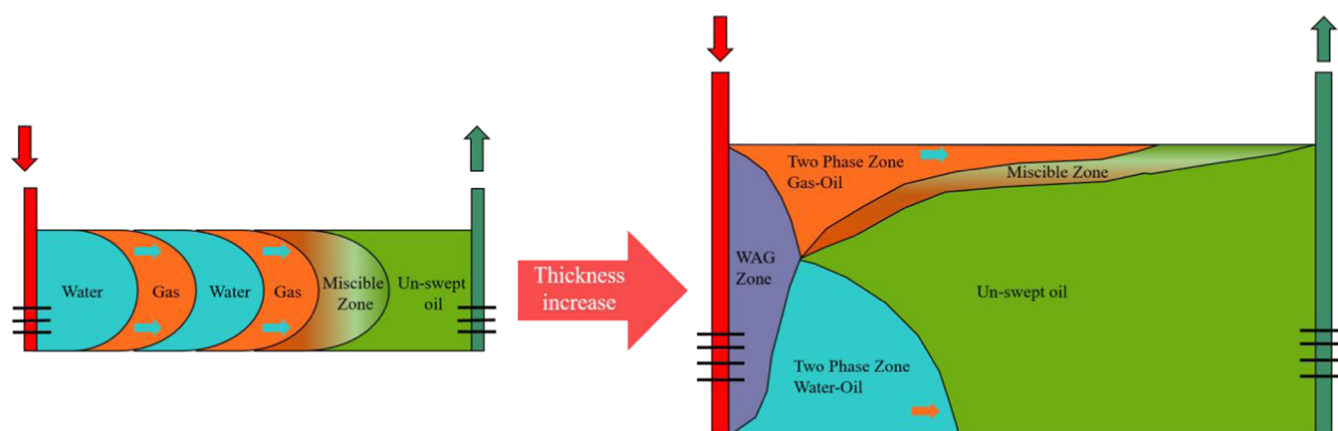
Figure 1. Comparative characteristics of water and gas migration in thin and thick reservoirs by using WAG injection.

Table 1. Studies of the Influencing Factors of WAG Flooding Using Reservoir Numerical Simulations

references	reservoir types	reservoir thickness (m)	type of gas	influencing factors
11	stratified sandstone reservoir	150	-	WAG ratio, injection rate, and cycling period
12	low-permeability sandstone reservoir	2.2	N_2	injection method, injection cycle, nitrogen injection volume, and WAG ratio
13	stratified sandstone heavy oil reservoir	-	CO_2	injection cycle, injection pressure, WAG ratio, and well fluid production rate
14	homogeneous oil reservoir mechanistic model	20	CO_2	wettability and relative permeability curve
15	ultra-low-permeability reservoir	11.4	CO_2	formation pressure, oil production rate, WAG time, GOR, and total gas injection volume
16	ultra-low-permeability reservoir	28.3	CO_2	WAG ratio, gas injection rate, WAG time, and WAG injection timing
17	homogeneous reservoir mechanistic model	10.6	CO_2	CO_2−WAG ratio
18,19	stratified heterogeneous carbonate reservoir	38.1−45.7	CO_2	dip angle, vertical permeability, gravity number mobility, horizontal permeability, anisotropy coefficient (K_V/K_H), and WAG ratio
20	homogeneous reservoir mechanistic model	3	CO_2	injection rate, segment plugging size, anisotropy coefficient (K_V/K_H), and well spacing/reservoir thickness (L/h)
21,22	low-permeability carbonate reservoir	0.6−3	HC, CO_2	WAG ratios, WAG start date, WAG duration, WAG timing, WAG cycle, production constraints, gas composition, and saturation pressure

gradually been utilized in the research on the evaluation of parameter importance in different domains.[28−30]

In summary, this study evaluates the geological factors affecting CO_2−WAG oil recovery in thick oil layers (>200 m) and their significance. Initially, the research reviews the current status of WAG technologies, identifying existing gaps. Subsequently, it incorporates a random forest algorithm to assess the importance of various factors and establishes the necessary fluid component and three-dimensional reservoir models. Through numerical simulation, this study investigates the impact of sedimentary rhythm, matrix permeability, high-permeability streaks (HPS), barrier layers, and dip angle on the effectiveness of CO_2−WAG oil recovery. Finally, the RF algorithm is used to rank the importance of geological factors. This study comprehensively examines multiple geological factors, providing a thorough assessment of the effectiveness of the CO_2−WAG injection technology. The findings offer valuable guidance and reference for optimizing the CO_2−WAG injection strategies under different geological conditions. Moreover, the ranking of geological factor importance derived from numerical simulations and random forest analysis offers data-driven decision support.

■ METHODS

Random Forest Importance Evaluation Method. Random forest (RF) is an ensemble learning method that uses bagging and random subspace techniques to obtain prediction results from multiple regression decision trees (DT).[31] RF can evaluate feature importance by calculating the prediction error rate on the out-of-bag data (OOB). If the OOB prediction error rate increases with the permutation value, it indicates the importance of the variable. The magnitude of the increase reflects the variable's importance for predicting the dependent variable.

Assuming there are M variables X_1, X_2,···, X_M, the statistical measure of the importance score of variable X_j is represented by VIM_j. The VIM_{ij} of variable X_j in the ith tree is as follows:

$$VIM_{ij} = \frac{\sum_{p=1}^{n_o^i} I(Y_p = Y_p^i)}{n_o^i} - \frac{\sum_{p=1}^{n_o^i} I(Y_p = Y_{p,\pi_j}^i)}{n_o^i} \quad (1)$$

where n_o^i is the number of observed examples in the OOB data of the ith tree; $I(x)$ is the indicator function, equaling 1 when the two values are equal and 0 otherwise; $Y_p \in \{0,1\}$ is the true result of the pth observation; $Y_p^i \in \{0,1\}$ is the predicted result of the pth observation in the ith tree before random

permutation; and $Y_{p,\pi_j}^i \in \{0,1\}$ is the predicted result of the pth observation in the ith tree after random permutation.

When variable X_j does not appear in the ith tree, VIM_{ij} is equal to 0.

The importance score of variable X_j in the RF is

$$VIM_j = \frac{\sum_{i=1}^{n} VIM_{ij}}{n} \tag{2}$$

where n is the number of classification trees in the RF.

Data Standardization. Data standardization is a crucial step before evaluating variable importance using an RF model. Z-score normalization is employed in this study. The formula for Z-score normalization is as follows

$$z = \frac{x - \mu}{\sigma} \tag{3}$$

where z represents the standardized and processed data, x denotes the original data, μ represents the mean of the data, and σ represents the standard deviation of the data.

MODEL ESTABLISHMENT

Fluid Component Model. To accurately simulate reservoir fluid behavior, we used crude oil from reservoir B

Table 2. Lumped Oil Components

pseudocomponents	mole fraction/%
CO_2	20.23
N_2C_1	37.52
C_{2+}	16.71
C_{6+}	10.86
C_{13+}	7.09
C_{29+}	4.14
C_{70+}	3.45

as the reference sample. Through component determination experiments, mole fractions of 24 components in the reference oil were obtained. For computational efficiency, we lumped these 24 components into 7 pseudocomponents (Table 2). The PVT model was then fitted based on these pseudocomponents, and the matching results are presented in Table 3.

Three-Dimensional Reservoir Numerical Model. To study the impact of geological factors on the CO_2−WAG process in thick reservoirs and understand the displacement process, we constructed a three-dimensional Cartesian grid model with dimensions of $22 \times 30 \times 20$, focusing on a typical thick reservoir (reservoir B). The grid had sizes of 100, 100, and 10 m in the X, Y, and Z directions, respectively. Gas injection from associated gas was utilized, and a two-injection and two-production well pattern was employed, alternating between gas injection and production (Figure 2). The parameter settings of the basic model are listed in Table 4.
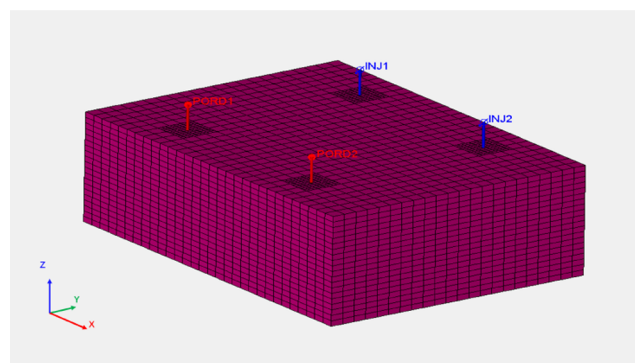

Figure 2. Three-dimensional reservoir numerical model for CO_2−WAG flooding.

ANALYSIS OF INFLUENCING FACTORS OF CO_2−WAG IN THICK RESERVOIRS

This work focuses on investigating the influence of geological factors in thick reservoirs on CO_2−WAG processes. The study aims to incorporate geological parameter settings and characterization while maintaining consistent injection and production parameters based on a homogeneous model.

Sedimentary Rhythm. Reservoir permeability exhibits various vertical changes due to multiple factors, such as the sedimentary environment, proximity of source materials, and mode of transportation. As shown in Figure 3, the sedimentary rhythm can be subdivided into seven types. Corresponding rhythm models are established based on these seven permeability rhythm types, with permeabilities ranging from 25 to 500 mD.

Combining the GOR rise curves, volumetric sweep efficiency, recovery results (Figure 4), and oil saturation profiles (Figure 5), it is evident that the transport and distribution of gas and water are significantly affected by the rhythm type due to gravity segregation and differential displacement velocity. Rhythm types with lower permeability in the upper reservoir section help suppress gas breakthrough, increase gas sweep, and slow the rate of GOR increase. On the other hand, rhythm types with good permeability in the lower reservoir section help increase water sweep and improve mobility control. Therefore, the adaptability of CO_2−WAG flooding for different sedimentary rhythm reservoirs can be ranked from strong to weak as follows: positive rhythm, compound negative−positive rhythm, compound positive rhythm, homogeneous rhythm, compound negative rhythm, compound positive−negative rhythm, and negative rhythm.

Dip Angle. To investigate the impact of dip angle on the efficacy of CO_2−WAG flooding for thick reservoirs, mechanistic models were constructed with dip angles of 0, 3, 6, 9, and 12° while keeping other parameters constant. The GOR rise curves, volumetric sweep efficiency, recovery results (Figure 6), and oil saturation profiles (Figure 7) were obtained. From Figure 6, it can be observed that a greater dip angle leads to a shorter gas breakthrough time in production wells and a faster

Table 3. Results of the Characterization of Oil Properties

property	measured data	PVT model matched data	error/%
$GOR/(sm^3/sm^3)$	206	207.515	0.735
oil density/(kg/m^3)	795	792.909	0.263
volume factor/(m^3/Sm^3)	1.48	1.476	0.27

Table 4. Reservoir Properties and Production Control Parameters of the Basic Model

reservoir properties	value	production control	value
thickness	200 m	WAG cycle	6 months
depth	5200 m	injection-to-production ratio	1
porosity	0.13	well spacing	1500 m
initial reservoir pressure	60 MPa	production period	30 years
horizontal permeability	300 mD	layer perforation	all 20 layers
anisotropy ratio (K_V/K_H)	0.1	injection gas	associated gas

(a)positive rhythm   (b)negative rhythm   (c)homogeneous rhythm
(d)compound positive rhythm   (e)compound negative rhythm
(f)compound positive-negative rhythm   (g)compound negative-positive rhythm
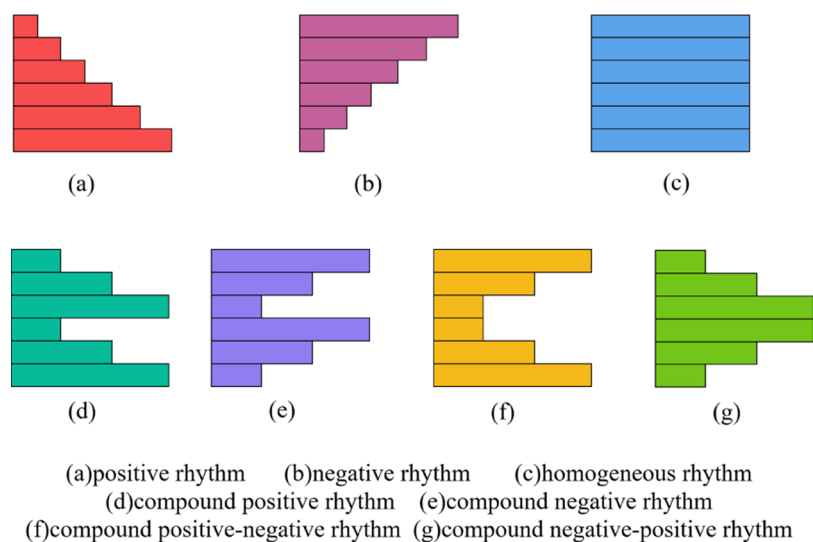
Figure 3. Different permeability rhythm types (the length of the rectangular strip reflects the magnitude of permeability).
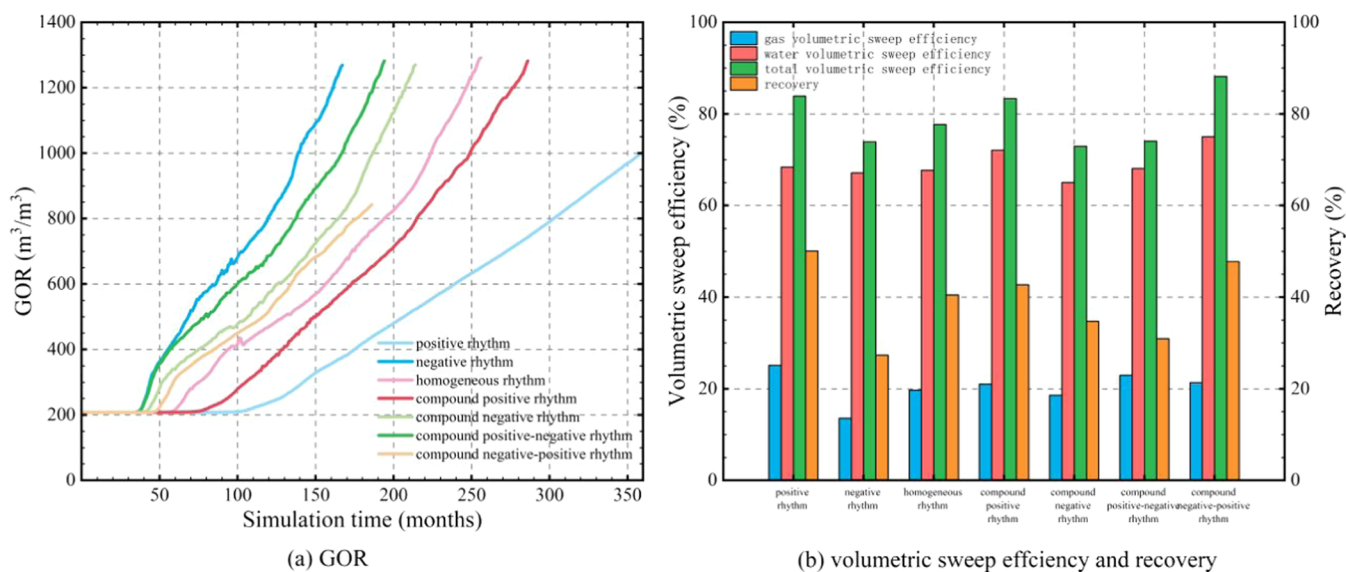
Figure 4. GOR rise curves, volumetric sweep efficiency, and recovery for different rhythm types.

(a) GOR

(b) volumetric sweep efficiency and recovery

increase in GOR. Figure 6 indicates that a larger dip angle results in an increase in the swept volume of gas but a decrease in the swept volume of water. Consequently, the overall swept volume decreases, and the remaining oil distribution area in the upper part of the reservoir, where no sweep has occurred, increases, leading to a decrease in recovery. This result demonstrates the combined effect of gravitational segregation and dip angle, which promotes the expansion of gas sweep while inhibiting water sweep. Therefore, when dealing with formations that have a dip angle, it is advisable to consider

increasing the WAG ratio to enhance the water sweep and achieve improved recovery.

Matrix Permeability. To investigate the impact of matrix permeability on the effectiveness of CO_2−WAG development in thick reservoirs, mechanistic models were established with matrix permeabilities of 100, 200, 300, 400, and 500 mD, with $K_V/K_H = 0.1$. As shown in Figure 8, an increase in matrix permeability leads to faster gas movement, resulting in an earlier gas breakthrough time at production wells but a slower rise in the gas−oil ratio. This is because the higher matrix
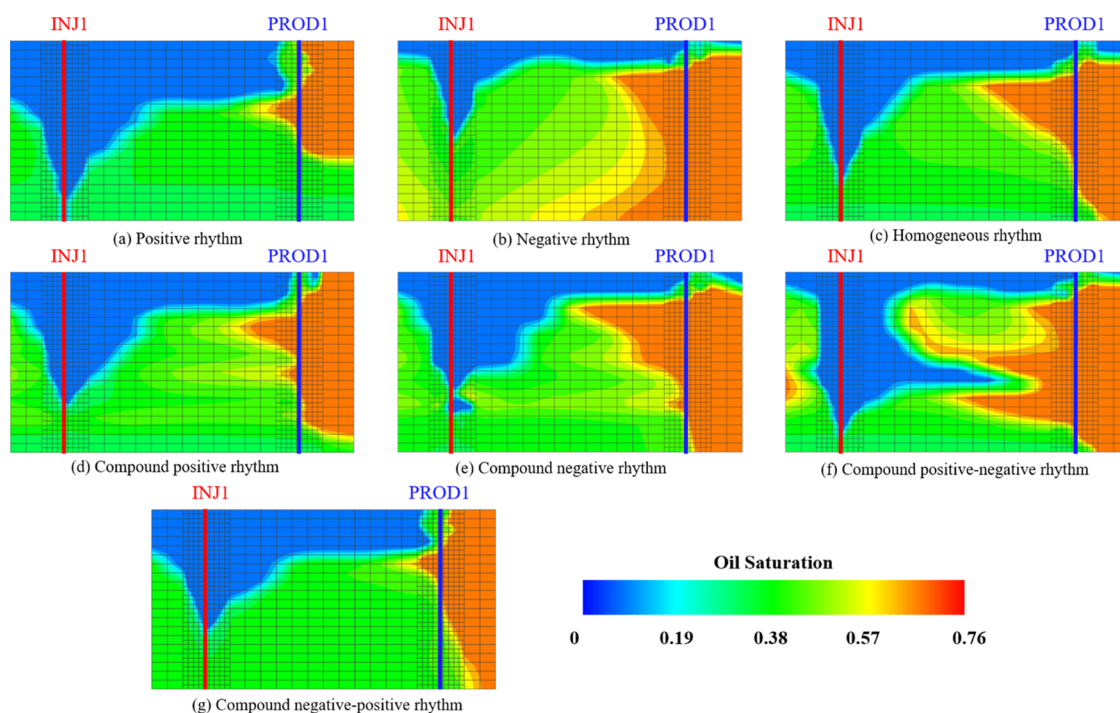
Figure 5. Oil saturation profiles for different rhythm types at the end of the simulation. GOR rise curves for different rhythm types.
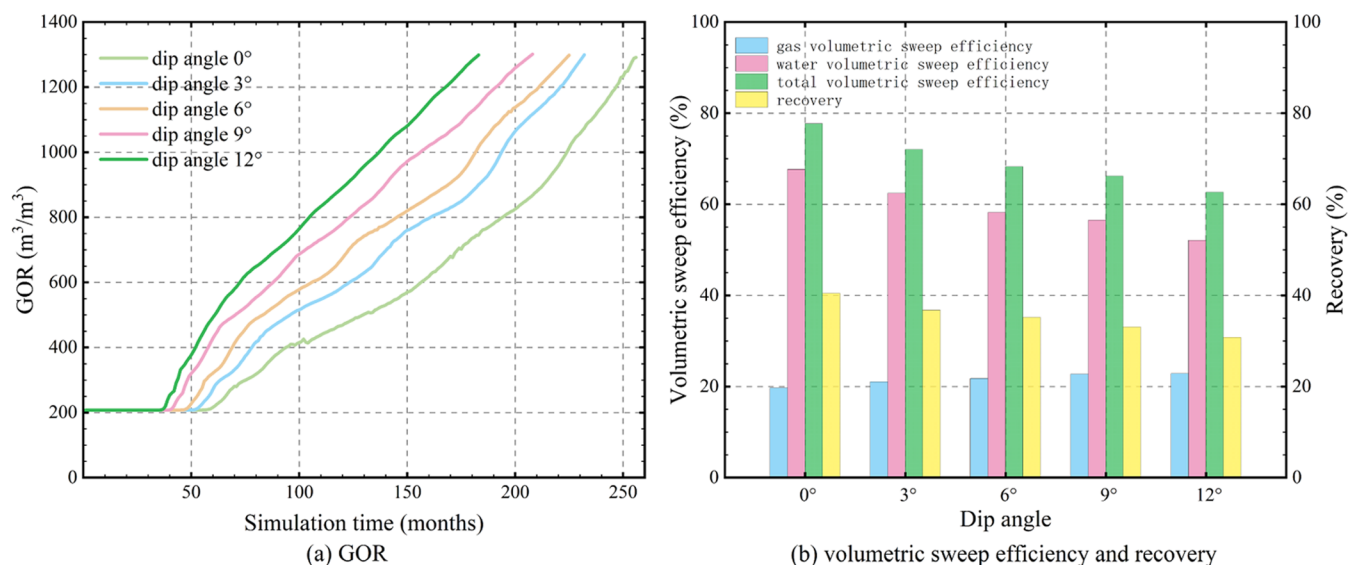

Figure 6. GOR rise curves, volumetric sweep efficiency, and recovery for different dip angles.

permeability causes the swept areas of gas and water to expand toward the edges, leading to a reduction in the unswept area (Figure 9). At the same time, there is a decrease in the gas that moves toward the production wells, leading to a slower increase in the gas–oil ratio, as shown in Figure 8. This results in an increased ability of water and gas to sweep the unswept area, leading to improved recovery.

High-Permeability Streaks (HPS). HPS refer to the portion of the reservoir with relatively higher permeability through which fluids preferentially flow. To analyze the impact of HPS with different distributions on CO_2–WAG flooding in thick reservoirs, models were set up with HPS located in the upper, middle, and lower sections.

Based on the GOR rise curves, volumetric sweep efficiency, recovery results (Figure 10), and oil saturation profiles (Figure

11), it can be observed that HPS accelerates the movement of water and gas. Combining this characteristic with the gravitational differentiation of water and gas, HPS at different locations have a significant influence on the distribution of water and gas movement. In the upper section, HPS cause a rapid breakthrough of injected gas, resulting in a sharp increase in the gas–oil ratio, early well shut-in, and extremely low recovery factor and sweep coefficient values. In the middle section, HPS facilitate the sweep of water and gas, especially in the middle part of the reservoir, delaying the gravitational differentiation of water and gas and improving the recovery factor and sweep coefficient. In the lower section, HPS lead to rapid water breakthrough, causing ineffective circulation of injected water, reducing water sweep, and decreasing the recovery factor. Therefore, the adaptability of the CO_2–WAG
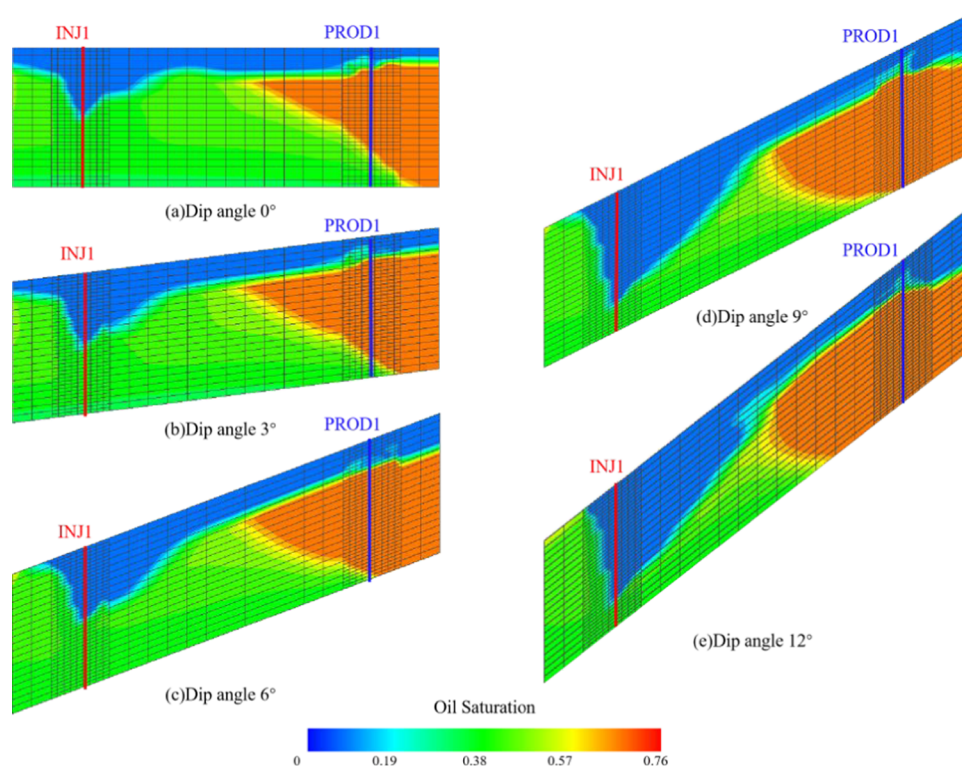
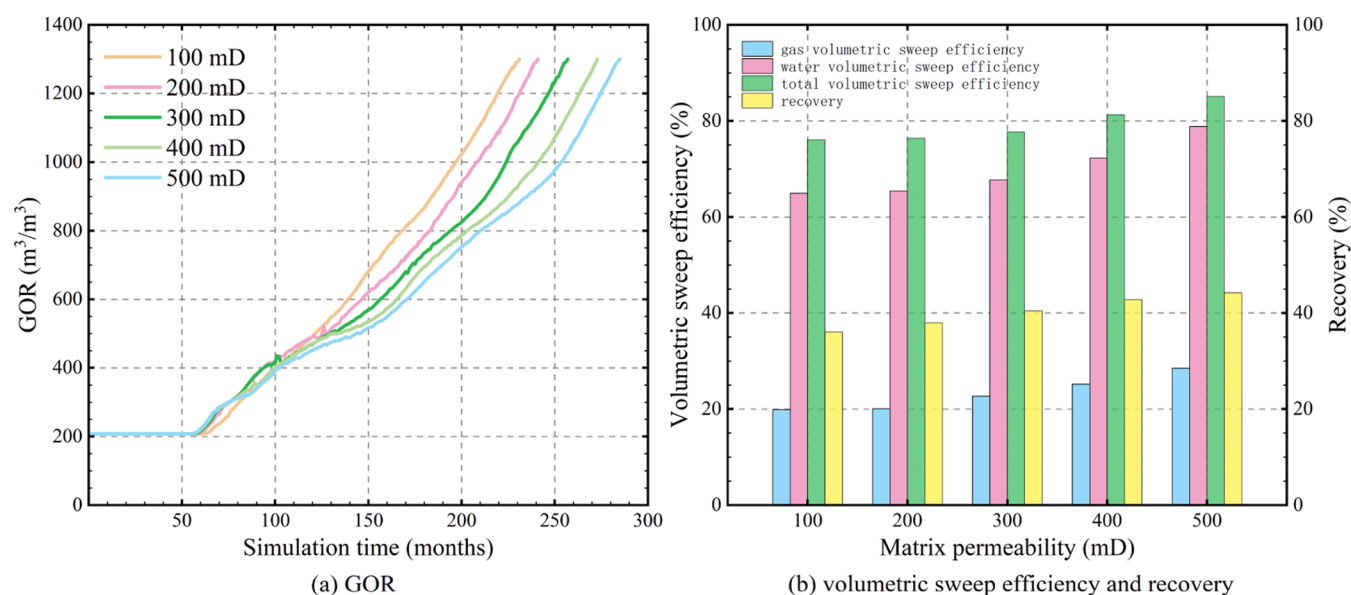**Figure 7.** Oil saturation profiles for different dip angles.

Figure 8. GOR rise curves, volumetric sweep efficiency, and recovery for different matrix permeability.

method to the distribution of HPS, from strong to weak, follows the order: middle section, homogeneous, lower section, and upper section.

Barrier Layers. The barrier layer refers to a low-permeability rock layer between oil layers. To clarify the effect of barrier layer distribution on CO_2−WAG development, three models with barrier layers located in the upper, middle, and lower sections are established.

From Figures 12(a) and 13, it can be seen that the impact of barrier layer distribution on GOR change during WAG flooding is minor, but it significantly affects the distribution of remaining oil. When the barrier layer is in the upper section,

most of the remaining oil is distributed in the middle section of the lower oil layer. With the barrier layer in the middle section, the remaining oil is distributed in the middle section of both upper and lower oil layers but in a relatively small area. When the barrier layer is in the lower section, most of the remaining oil is distributed in the middle section of the upper oil layer. Figure 12(b) compares sweeping efficiency and recovery factor under different barrier layer distributions, indicating that the effect of a single barrier layer distribution on CO_2−WAG development is relatively small within the simulation scale of this study.
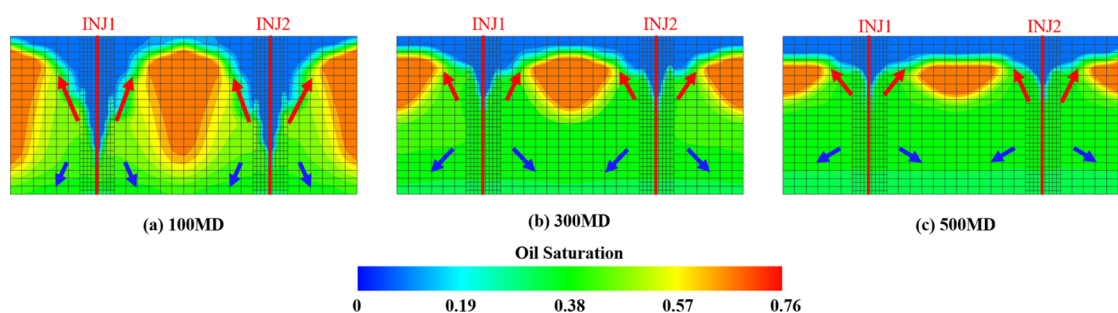
Figure 9. Oil saturation profiles for different matrix permeability in the x direction (the red arrow indicates the direction of gas migration, and the blue arrow indicates the direction of water migration).
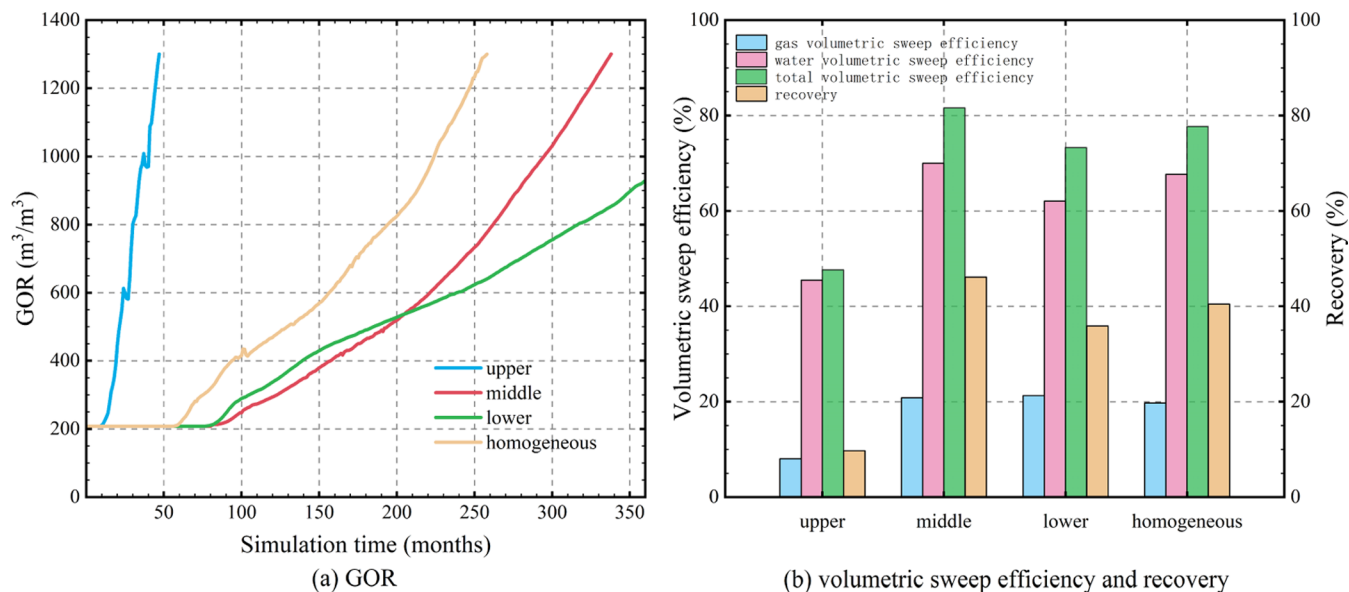

Figure 10. GOR rise curves, volumetric sweep efficiency, and recovery for different HPS distributions.

Table 5. Calculation Results of the RF Importance Evaluation Algorithm

no.	random seed	HPS	sedimentary rhythm	dip angle	matrix permeability	barrier layer
1	298	0.4842	0.2358	0.1943	0.0767	0.0091
2	241	0.5364	0.2270	0.1728	0.0513	0.0125
3	162	0.5725	0.2092	0.1528	0.0494	0.0161
4	112	0.4694	0.2499	0.1949	0.0595	0.0263
5	475	0.5104	0.2329	0.1815	0.0569	0.0183
6	79	0.5529	0.2334	0.1550	0.0451	0.0137

◼ EVALUATING IMPORTANCE USING RF

To construct an RF model, this study established a database consisting of 504 numerical simulation models of reservoirs through a combination of multiple-factor experiments. The database was split into a training set (70%) and a testing set (30%). Five geological factors influencing CO_2−WAG flooding were used as input variables for the model, with the recovery factor as the prediction target. The RF algorithm is characterized by randomness. To ensure the reproducibility of the computational results, six feature importance calculations were conducted by setting different random seeds (Table 5), and the factors were ranked based on the average importance scores.

Based on the average importance scores of the influencing factors obtained from the RF calculations (Figure 14), it can be observed that the importance levels of the geological factors, from highest to lowest, are HPS, sedimentary rhythm, dip angle, matrix permeability, and barrier layer. Therefore, in the early design of CO_2−WAG strategies for thick reservoirs with alternating water and gas injection, priority should be given to considering the impact of HPS, sedimentary rhythm, and dip angle on reservoir development. This involves selecting reservoir areas with stronger adaptability for implementing CO_2−WAG flooding or proposing targeted measures to improve development effectiveness.

◼ RESULTS AND DISCUSSION

The research results demonstrate that geological factors significantly impact the flooding of CO_2−WAG in thick reservoirs. Sedimentary rhythm affects injected water and gas distribution and recovery factor, with positive rhythm being the most effective. The dip angle intensifies gravity segregation, shortening gas breakthrough time and decreasing the swept
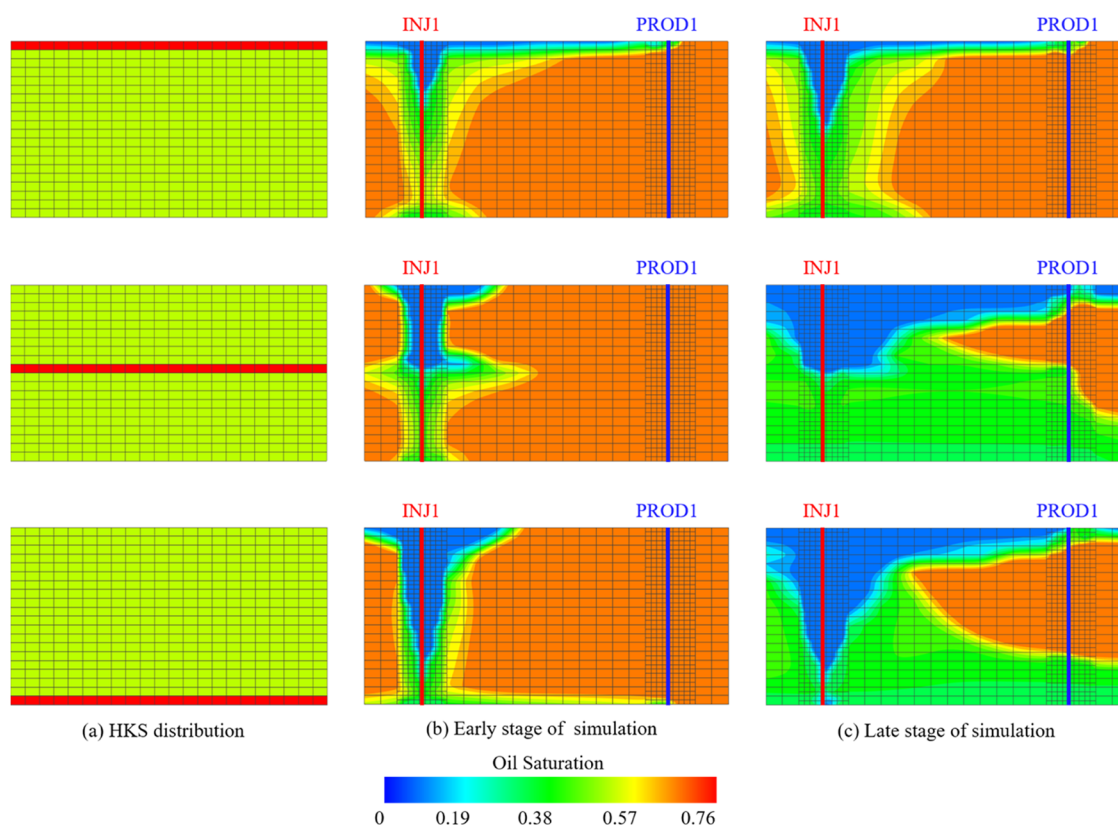
Figure 11. Oil saturation profiles for different HPS distributions at early and late stages of the simulation.
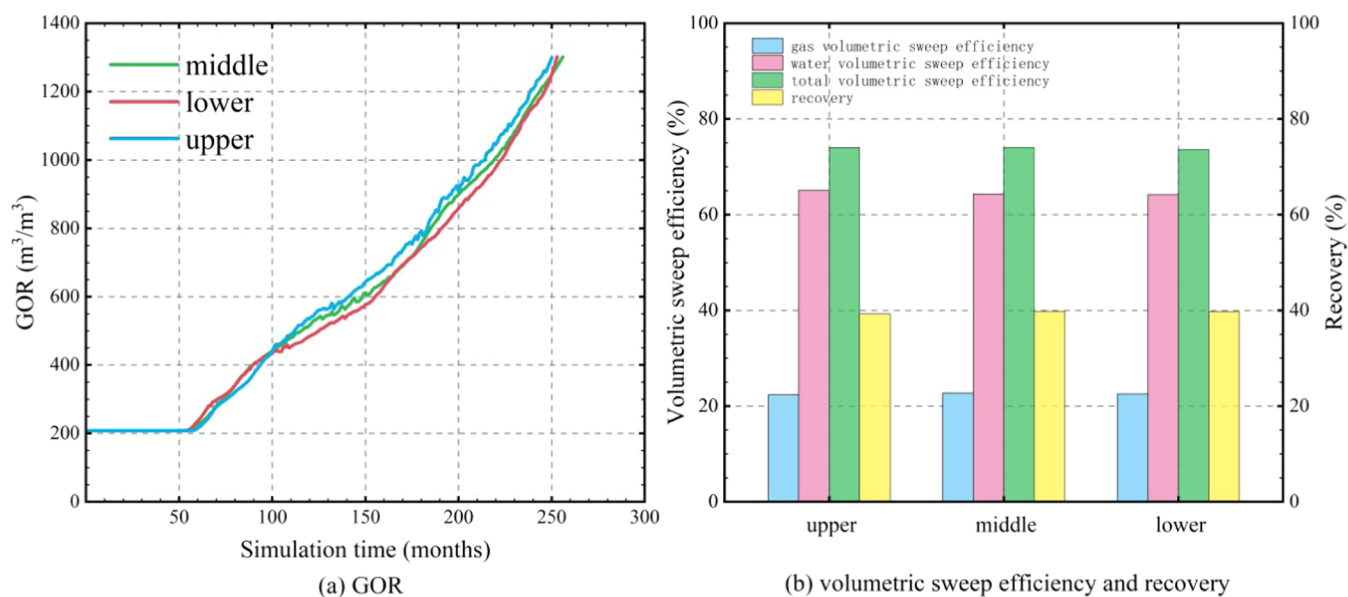

Figure 12. GOR rise curves, volumetric sweep efficiency, and recovery for different barrier layer distributions.

area and recovery factor. Increasing matrix permeability expands water and gas sweep and improves the recovery factor. HPS at the upper part result in poor performance, while in the middle, they are favorable for water and gas sweep and increase the recovery factor. A single barrier layer has a relatively small impact on CO_2−WAG flooding. HPS are the most important geological factor, followed by sedimentary rhythm, dip angle, matrix permeability, and barrier layer.

Although the random forest algorithm and numerical simulations have provided valuable insights into the CO_2−

WAG flooding technique, the general applicability of this study's results needs further validation in actual oilfield operations. Future research will continue to optimize injection and production parameters based on geological factors, seeking the optimal match between geological and dynamic factors.

■ ASSOCIATED CONTENT

Data Availability Statement

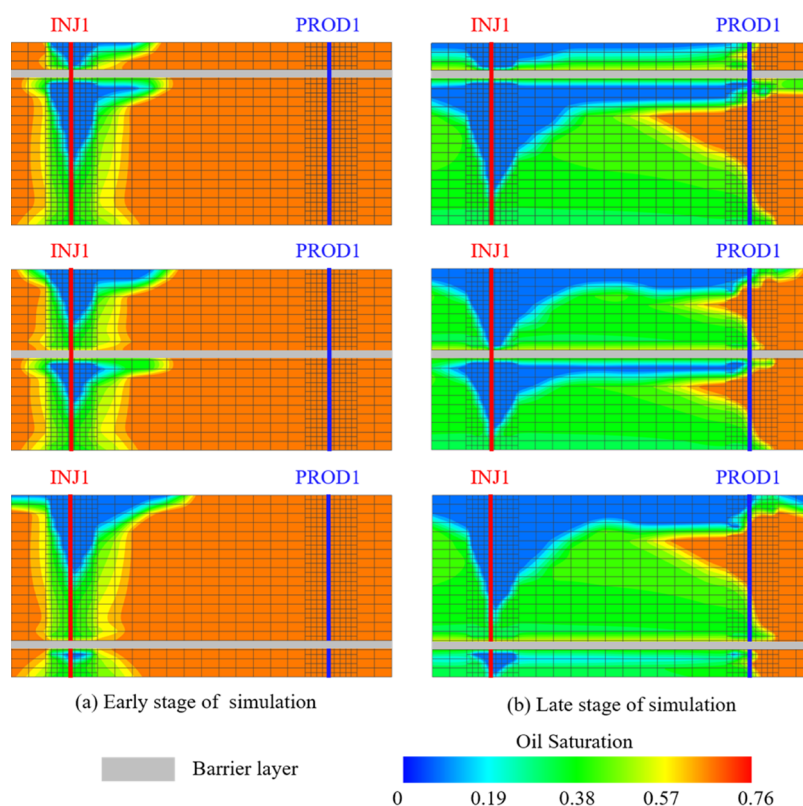All data referenced in this paper are openly available. Further information can be obtained by contacting the authors.

(a) Early stage of simulation

(b) Late stage of simulation

Oil Saturation

Barrier layer

0   0.19   0.38   0.57   0.76

Figure 13. Oil saturation profiles for different barrier layer distributions at the early and late stages of the simulation.
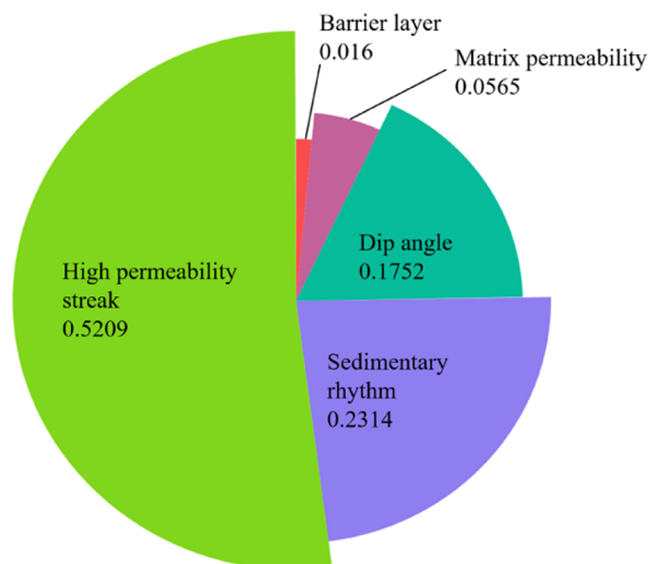

Figure 14. Average importance score of each influence parameter derived from the RF importance evaluation algorithm.

AUTHOR INFORMATION

Corresponding Author

Yunbo Li − *PetroChina, Research Institute of Petroleum Exploration and Development, Beijing 100083, China;* orcid.org/0009-0008-5490-2233; Email: 3189009871@qq.com

Authors

Qiang Luo − *PetroChina, Research Institute of Petroleum Exploration and Development, Beijing 100083, China;* orcid.org/0009-0000-5188-6591

Hao Sun − *PetroChina, Research Institute of Petroleum Exploration and Development, Beijing 100083, China*

Shangqi Liu − *PetroChina, Research Institute of Petroleum Exploration and Development, Beijing 100083, China*

Yang Yu − *PetroChina, Research Institute of Petroleum Exploration and Development, Beijing 100083, China;* orcid.org/0000-0003-1196-000X

Zhaopeng Yang − *PetroChina, Research Institute of Petroleum Exploration and Development, Beijing 100083, China*

Complete contact information is available at:
https://pubs.acs.org/10.1021/acsomega.4c04901

Notes

The authors declare no competing financial interest.

ACKNOWLEDGMENTS

NOMENCLATURE

WAG   water alternating gas

HPS   high-permeability streaks
SBPSC   Santos Basin Pre-Salt Cluster
WF   water flooding
GI   gas injection
GOR   gas—oil ratio
PVT   pressure, volume, and temperature
RF   random forest
DT   decision trees
OOB   out-of-bag data
VIM   variable importance measures

◼ REFERENCES

(1) Wang, G. *Oil and Gas Exploration and Development Practice in Deepwater Brazil*; Petroleum Industry Press, 2020.

(2) Beltrao, R. L. C.; Sombra, C. L.; Lage, A. C. V. M.; Netto, J. R. F.; Henriques, C. C. D. *SS: Pre-Salt Santos Basin - Challenges and New Technologies for the Development of the Pre-Salt Cluster*, OnePetro, Santos Basin, Brazil, 2009. DOI: DOI: 10.4043/19880-MS.

(3) Filho, F. G. R. V.; Naveiro, J. T.; De Oliveira, A. P. Developing Mega Projects Simultaneously: The Brazilian Pre-Salt Case. In *All Days*; OTC: Houston, Texas, USA, 2015; p OTC-25896-MS. DOI: 10.4043/25896-MS.

(4) Vieira, R. A. M.; Cardoso, M. A.; Pizarro, J. O. S. *An Integrated WAG Characterization Study for an Offshore Oilfield*; OnePetro, 2019 DOI: 10.4043/29766-MS.

(5) Afzali, S.; Rezaei, N.; Zendehboudi, S. A Comprehensive Review on Enhanced Oil Recovery by Water Alternating Gas (WAG) Injection. *Fuel* 2018, 227, 218—246.

(6) Samba, M. A.; Elsharafi, M. O. Literature Review of Water Alternation Gas Injection. *J. Earth Energy Eng.* 2018, 7 (2), 33—45.

(7) Christensen, R.; Stenby, E. H.; Skauge, A. Review of WAG Field Experience. 2001, 10. DOI: DOI: 10.2118/71203-PA.

(8) Leach, M. P.; Yellig, W. F. Compositional Model Studies − CO2 Oil-Displacement Mechanisms. *SPE J.* 1981, 21 (01), 89—97.

(9) Clancy, J. P.; Gilchrist, R. E.; Cheng, L. H. K.; Bywater, D. R. Analysis of Nitrogen-Injection Projects to Develop Screening Guides and Offshore Design Criteria. *J. Pet. Technol.* 1985, 37 (06), 1097—1104.

(10) Green, D. W.; Willhite, G. P. *Enhanced Oil Recovery*; Society of Petroleum Engineers, 2018; Vol. 6 DOI: 10.2118/9781613994948.

(11) Drid, N.; Tiab, D. The Performance of WAG in a Stratified Reservoir, Hassi-Messaoud Field, OnePetro, Algeria, 2004 DOI: 10.2118/88482-MS.

(12) Guo, Q.; Liu, Y.; Fu, C. Study on Optimization of Nitrogen Injection Parameters and Nitrogen Injection Scheme for Water-Gas Alternation in Huang 16 Well Area. *J. Oil Gas Technol.* 2004, No. 03, 104—105 + 8.

(13) Fu, M.; Ye, C.; Xiong, F.; Ding, Z. Parameter Optimization and Scheme Design of CO2 Flooding in Block T34. *Drill. Prod. Technol.* 2011, 34 (01), 56—58 + 116.

(14) Faisal, A.; Bisdom, K.; Zhumabek, B.; Mojaddam Zadeh, A.; Rossen, W. R. Injectivity and Gravity Segregation in WAG and SWAG Enhanced Oil Recovery. In *All Days*; SPE: New Orleans, LA, 2009; p SPE-124197-MS. DOI: 10.2118/124197-MS.

(15) Wang, H.; Liao, X.; Zhao, X. Optimization of CO2 Flooding Parameters in Ultra-Low Permeability Reservoirs. *J. Southwest Pet. Univ., Sci. Technol. Ed.* 2014, 36 (06), 95—104.

(16) Li, M.; Guan, H.; Hu, S.; Wang, X.; Li, Q.; Yuan, S. Optimization of Water-Gas Alternating Injection-Production Parameters for CO2 Miscible Flooding and Immiscible Flooding in Ultra-Low Permeability Reservoirs. *Uncon. Oil Gas* 2021, 8 (01), 60—66.

(17) Abdurrahman, M.; Hidayat, F.; Husna, U. Z.; Arsad, A. Determination of Optimum CO2 Water Alternating Gas (CO2-WAG) Ratio in Sumatera Light Oilfield. *Mater. Today: Proc.* 2021, 39, 970—974.

(18) Khan, M. Y.; Mandal, A. The Impact of Permeability Heterogeneity on Water-Alternating-Gas Displacement in Highly Stratified Heterogeneous Reservoirs. *J. Pet. Explor. Prod. Technol.* 2022, 12 (3), 871—897.

(19) Khan, M. Y.; Mandal, A. Analytical Model of Incremental Oil Recovery as a Function of WAG Ratio and Tapered WAG Ratio Benefits over Uniform WAG Ratio for Heterogeneous Reservoir. *J. Pet. Sci. Eng.* 2022, 209, No. 109955.

(20) Darvish Sarvestani, A.; Rostami, B. Impact of Proper Design of Operating Parameters on the Performance of CO2 -Water Alternating Gas (CO2 -WAG) Injection: A Simulation Study. *Pet. Sci. Technol.* 2022, 40 (10), 1258—1277.

(21) Pal, M. Water Alternating Gas (WAG) Recovery Process Evaluation through Simulation for a Giant Middle-Eastern Carbonate Reservoir. *Pet. Sci. Technol.* 2022, 40 (10), 1233—1257.

(22) Pal, M.; Pedersen, R. B.; Gilani, S. F.; Tarsauliya, G. *Challenges and Learnings from Operating the Largest Off-Shore WAG in the Giant Al-Shaheen Field and Ways to Optimize Future WAG Developments*; OnePetro, 2018 DOI: 10.2118/190343-MS.

(23) Kuang, L.; Liu, H.; Ren, Y.; Luo, K.; Shi, M.; Su, J.; Li, X. Application and Development Trend of Artificial Intelligence in Petroleum Exploration and Development. *Pet. Explor. Dev.* 2021, 48 (1), 1—11.

(24) Breiman, L. Random Forests. *Mach. Learn.* 2001, 45 (1), 5—32.

(25) Strobl, C.; Boulesteix, A.-L.; Zeileis, A.; Hothorn, T. Bias in Random Forest Variable Importance Measures: Illustrations, Sources and a Solution." BMC Bioinformatics, 8(1), 25. *BMC Bioinf.* 2007, 8, 25.

(26) Calle, M. L.; Urrea, V. Letter to the Editor: Stability of Random Forest Importance Measures. *Briefings Bioinf.* 2011, 12 (1), 86—89.

(27) Boulesteix, A.-L.; Bender, A.; Lorenzo Bermejo, J.; Strobl, C. Random Forest Gini Importance Favours SNPs with Large Minor Allele Frequency: Impact, Sources and Recommendations. *Briefings Bioinf.* 2012, 13 (3), 292—304.

(28) Zhao, Y.; Zhu, W.; Wei, P.; Fang, P.; Zhang, X.; Yan, N.; Liu, W.; Zhao, H.; Wu, Q. Classification of Zambian Grasslands Using Random Forest Feature Importance Selection during the Optimal Phenological Period. *Ecol. Indic.* 2022, 135, No. 108529.

(29) Grekousis, G.; Feng, Z.; Marakakis, I.; Lu, Y.; Wang, R. Ranking the Importance of Demographic, Socioeconomic, and Underlying Health Factors on US COVID-19 Deaths: A Geographical Random Forest Approach. *Health Place* 2022, 74, No. 102744.

(30) Hwang, S.-W.; Chung, H.; Lee, T.; Kim, J.; Kim, Y.; Kim, J.-C.; Kwak, H. W.; Choi, I.-G.; Yeo, H. Feature Importance Measures from Random Forest Regressor Using Near-Infrared Spectra for Predicting Carbonization Characteristics of Kraft Lignin-Derived Hydrochar. *J. Wood Sci.* 2023, 69 (1), 1.

(31) Cutler, A.; Cutler, D. R.; Stevens, J. R. Random Forests. In *Ensemble Machine Learning: Methods and Applications*; Zhang, C.; Ma, Y., Eds.; Springer: New York, NY, 2012; pp 157—175 DOI: 10.1007/978-1-4419-9326-7_5.